BIOCHEMISTRY
including biophysical chemistry & molecular biology

Article

pubs.acs.org/biochemistry

Zn(II) Stimulation of Fe(II)-Activated Repression in the Iron-Dependent Repressor from *Mycobacterium tuberculosis*

Brian Stapleton,[†] Lawrence R. Walker,[†] and Timothy M. Logan*[,†,‡]

[†]Department of Chemistry and Biochemistry, 102 Varsity Way, Florida State University, Tallahassee, Florida 32306-4390, United States

[‡]Graduate Program in Molecular Biophysics, 91 Chieftan Way, Florida State University, Tallahassee, Florida 32306-4380, United States

ABSTRACT: Thermodynamic measurements of Fe(II) binding and activation of repressor function in the iron-dependent repressor from *Mycobacterium tuberculosis* (IdeR) are reported. IdeR, a member of the diphtheria toxin repressor family of proteins, regulates iron homeostasis and contributes to the virulence response in *M. tuberculosis*. Although iron is the physiological ligand, this is the first detailed analysis of iron binding and activation in this protein. The results showed that IdeR binds 2 equiv of Fe(II) with dissociation constants that differ by a factor of 25. The high- and low-affinity iron binding sites were assigned to physical binding sites I and II, respectively, using metal binding site mutants. IdeR was also found to contain a high-affinity Zn(II) binding site that was assigned to physical metal binding site II through the use of binding site mutants and metal competition assays. Fe(II) binding was modestly weaker in the presence of Zn(II), but the coupled metal binding−DNA binding affinity was significantly stronger, requiring 30-fold less Fe(II) to activate DNA binding compared to Fe(II) alone. Together, these results suggest that IdeR is a mixed-metal repressor, where Zn(II) acts as a structural metal and Fe(II) acts to trigger the physiologically relevant promoter binding. This new model for IdeR activation provides a better understanding of IdeR and the biology of iron homeostasis in *M. tuberculosis*.

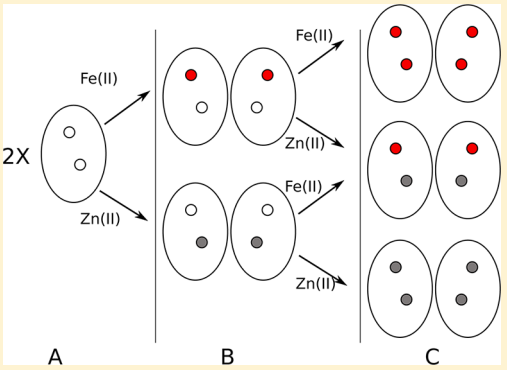

According to the Centers for Disease Control and Prevention and the World Health Organization, nearly one-third of the world's population is infected with *Mycobacterium tuberculosis*, with roughly 10% of them exhibiting active infection.[1] The virulence of *M. tuberculosis* is controlled at the molecular level by several factors, including the availability of ferrous iron. The iron-dependent regulator (IdeR) is an important Fe(II) sensor and virulence regulator in *M. tuberculosis*.[2] IdeR is a member of the diphtheria toxin repressor (DtxR) family of iron-dependent repressors, which regulate the expression of large families of genes, including virulence genes, by binding divalent iron, thereby repressing gene expression at high levels of iron and derepressing gene expression at low levels of iron. IdeR has been proposed to regulate expression of approximately 45 genes in *M. tuberculosis*, including several virulence factors, iron homeostasis genes, and oxidative stress genes.[3−6] IdeR homologues are found in several species, including *Corynebacterium diphtheriae*,[7] and orthologues are present in all *Mycobacterium* species.[3] Interestingly, IdeR deletion is lethal to virulent species of *Mycobacterium* such as *M. tuberculosis* but not to nonvirulent species such as *Mycobacterium smegmatis*.[8] Furthermore, IdeR expression is upregulated in *M. tuberculosis* isolated from mouse macrophages.[9]

Structural and functional studies of IdeR, DtxR, and other DtxR family members have led to the following model for metal activation. IdeR exists as a loosely associated dimer of molten globule-like monomers in the apo or low-metal state.[10] This state is incapable of sequence-specific recognition of promoter sites. Metal binding induces a transition to a more ordered structure, enhances dimer formation, and optimally orients the DNA-binding helix in each monomer for DNA binding. An IdeR dimer binds to DNA, while a second IdeR dimer binds the opposite side of the same promoter, forming a dimer−dimer DNA complex (Figure 1). This model accounts for much of the known biophysics of IdeR but fails to explain some of the outstanding questions with regard to IdeR biology, such as metal selectivity. Given the importance of Fe(II) binding in these regulators, it is surprising that only a few studies of IdeR or DtxR biophysics have used Fe(II) as the activating metal. Spiering et al.[11] used a surface plasmon resonance-like method to determine that DtxR binds 2 equiv of Fe(II) under saturating conditions (similar to that of other divalent transition metals) but were unable to determine the energetics of binding. Chou et al.[12] used a coupled metal-DNA binding assay to show that Fe(II) was a better activator of DNA binding than Ni(II) or Co(II), but the Fe(II)-activated form had an affinity for

Received: November 30, 2012
Revised: January 19, 2013
Published: February 22, 2013

   dx.doi.org/10.1021/bi301608p | *Biochemistry* 2013, 52, 1927−1938

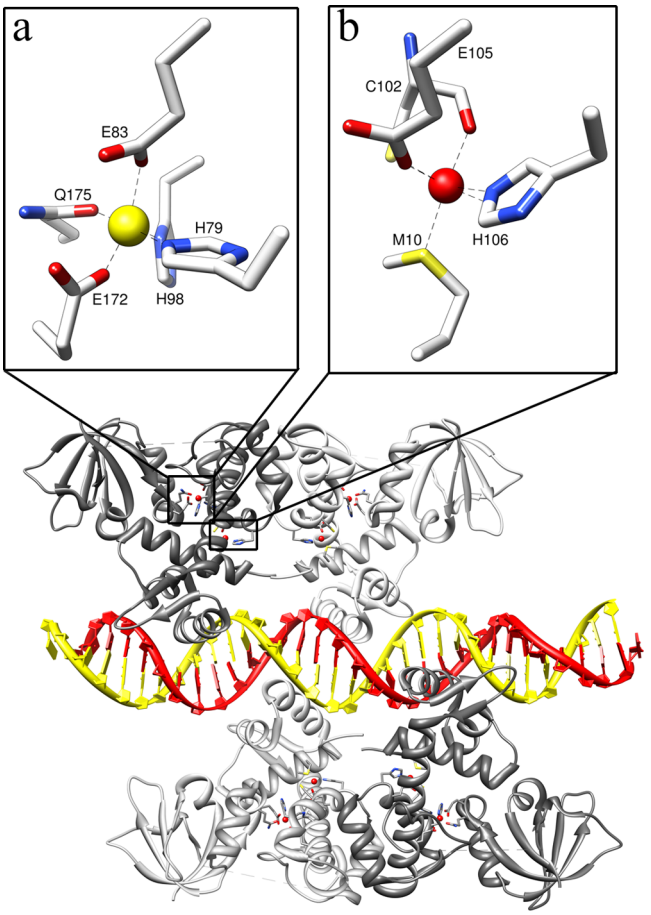

Figure 1. Crystal structure of IdeR. Crystal structure of two dimers of IdeR bound to the *mbtA*–*mbtB* DNA promoter sequence. Metal coordination shown for (a) site I residues and (b) site II residues. Structures generated from PDB entry 1U8R.[31] Images created using UCSF Chimera.[11]

promoter binding lower than those seen in other metal-responsive regulators.[13−15]

Consequently, the basis for metal selectivity in the DtxR family of proteins is an unresolved question,[16] primarily because there have been no detailed studies of iron binding or iron activation of promoter binding. IdeR has two structurally and functionally distinct metal binding sites per monomer (Figure 1). These sites are located in the larger of the two domains in IdeR, which also contains the DNA binding motif and the dimer interface. The smaller, C-terminal domain may also contribute to metal binding by completing the coordination of one of the two sites. These sites are termed sites I and II[17] or the ancillary and primary sites,[18] respectively. Site I, which was most consistently occupied by metal in the early crystal structures (leading to its designation as site I), is formed by the side chains of residues H79, E83, H98, E172, and Q175 and coordinates metal in a distorted trigonal bipyramidal geometry (Figure 1a). Site II is formed by side chains of residues M10, C102, E105, and H106, the carboxyl group of C102, and a water molecule and coordinates metal in a distorted octahedral geometry (Figure 1b). Single mutations to residues in site I reduce repressor function, whereas single-site mutations to site II abolish repressor activity, leading to the alternative but more functionally descriptive designation as ancillary and primary sites, respectively.[18] Given the difference in coordinating ligands and geometry, it is not immediately obvious that both sites would bind Fe(II) or what the metal binding energetics might be. Indeed, the in vivo metal specificity of DtxR was changed to Mn(II) rather than Fe(II) via introduction of the M10D and C102E mutations[19] into site II, suggesting that there may be more to metal selectivity than was apparent from the previous biophysical studies.

We hypothesized that Fe(II) selection could result from a higher affinity for Fe(II) than for other metals, from more cooperative binding of Fe(II) than of other metals, or a combination of both. We tested this idea using a combination of equilibrium dialysis experiments to measure Fe(II) binding energetics and a fluorescence anisotropy-based assay to correlate the metal activation to promoter binding. Fe(II) oxidation was minimized by using *N*-acetylcysteine (NAC) as a reducing agent. NAC has a lower reduction potential than dithiothreitol (DTT)[20,21] but is the functional end of mycothiol, the reducing agent found in *Mycobacterium* species.[22] Metal binding and promoter activation were evaluated for several divalent transition metals that are known to activate promoter binding in vitro.[7] The data showed that the thermodynamics of Fe(II) binding and repressor activation are significantly different from those of other metals, except Zn(II). The results led us to investigate whether Fe(II) binding and activation in IdeR could depend on a mixture of metal species, similar to that seen in Fur, the other major bacterial Fe(II) sensor.

MATERIALS AND METHODS

Expression and Purification. IdeR was expressed in *Escherichia coli* BL21(DE3) cells grown in Terrific Broth medium using an autoinduction protocol.[23] Cells were pelleted and resuspended in nickel buffer A [50 mM sodium phosphate (pH 6.8) and 40 mM NaCl] and lysed using a microfluidizer (Microfluidics Corp., Newton, MA). The lysate was clarified by centrifugation at 48400x *g* and loaded onto a Ni-NTA HisTrap column (GE Biosciences, Piscataway, NJ) equilibrated with nickel buffer A. The nickel affinity column was washed with 10 column volumes of nickel buffer A, and the protein was eluted with nickel buffer B [20 mM sodium phosphate (pH 7.4), 500 mM NaCl, and 50 mM EDTA]. Fractions containing the most pure IdeR were pooled, concentrated, exchanged into 50 mM Tris (pH 8.5), and loaded onto a HiTrap Q-Sepharose anion-exchange column (GE Biosciences). Bound protein was eluted with a NaCl gradient from 0 to 2 M. The highest-purity fractions were pooled, concentrated, brought to 20 mM ethylenediaminetetraacetic acid (EDTA), and exchanged into 10 mM MES buffer (pH 6.8) in the presence of Chelex 100 (Bio-Rad, Hercules, CA). The protein was concentrated and aliquoted into 3 mL fractions and frozen at −80 °C. The protein concentration was measured on a Cary 300 spectrometer (Varian Inc., Palo Alto, CA) in the presence of 6 M urea at 280 nm and calculated using an estimated extinction coefficient of 13980 cm^{-1} M^{-1} (http://www.expasy.org). Protein prepared in this way could be stored frozen at −80 °C for up to 3 months prior to use with no loss of activity.

Expression and Purification of Mutants. IdeR mutants were expressed as described above with the addition of a second anion-exchange column after protein was diluted 2-fold with 50 mM Tris (pH 8.5). All other steps were performed exactly as described above for wild-type IdeR.

Activation for Metal Binding. IdeR contains a single Cys residue that slowly forms intermonomer disulfide bonds that

inactivate the protein. Prior to metal binding experiments, the disulfide was reduced by treatment with 5 mM tris(2-carboxyethyl)phosphine (TCEP) for 2 h at room temperature. TCEP was removed by passing the sample through a HiTrap desalting column (GE Biosciences) at a rate of 1 mL/min and exchanging the buffer with metal-free 10 mM MES (pH 6.8). The free thiol content of reduced IdeR was quantified using Ellman's reagent. In the experiments reported here, the ratio of free cysteine to IdeR monomer averaged 0.98 (the expected number is 1), with no change in this ratio following the metal binding experiments. Only samples with thiol:IdeR ratios of >0.95 or <1.05 were used for subsequent experiments. The glassware used for all experiments involving reduced and activated protein was demetalated by being soaked in 20% nitric acid and rinsed thoroughly with Nanopure water.

Equilibrium Dialysis Studies. Equilibrium dialysis experiments were performed at 25 °C using 2 mL, two-chamber dialysis cells (Bel-Art Scienceware, Pequannock, NJ) separated by a demetalated 3500 Da molecular mass cutoff dialysis membrane. The membranes were rinsed initially with Nanopure purified water and then soaked in Chelex-100-treated 10 mM MES buffer (pH 6.8) prior to the experiment. In each experiment, 800 μL of active, demetalated protein at a concentration of 30 μM was added to one side of the dialysis membrane and 800 μL of a solution containing protein free metal at twice the final concentration was added to the other chamber. The buffers in both chambers consisted of 10 mM MES, 100 mM NaCl, and 2 mM *N*-acetylcysteine (NAC) (pH 6.8). The metal solutions were prepared using ICP-MS metal standards (Sigma-Aldrich, St. Louis, MO). The loaded cells were allowed to equilibrate on a rotating shaker for ∼18 h at room temperature. The final concentration of Fe(II), Mn(II), Zn(II), and Ni(II) from each chamber was determined using 2,2′,2″-terpyridine (terpy), which exhibits characteristic absorption bands between 320 and 700 nm when bound to metal.[24] The samples were adjusted to 5 M urea to ensure release of metal, and terpy was added to a final concentration of 330 μM prior to measurement. The amount of metal in each sample was derived from the peak absorbance at the spectral maximum for the specific metal−terpy complex based on a standard curve generated using identical sample conditions. The fraction bound at each metal concentration, *r*, was calculated as

$$r = \frac{M^{2+}_{\text{total}} - M^{2+}_{\text{free}}}{P_{\text{total}}} \quad (1)$$

where M^{2+}_{total} is the metal concentration from the protein chamber, M^{2+}_{free} is the metal concentration from the metal solution chamber, and P_{total} is the protein concentration from the protein chamber.

Simultaneous Binding Curves for Multiple Metal Species. Samples for inductively coupled plasma mass spectrometry (ICP-MS) analysis were gravimetrically dissolved in 2% HNO_3 prepared using Optima grade HNO_3 (Sigma-Aldrich) and 18.3 MΩ (Thermo Fisher, Waltham, MA) water under Class 100 clean lab conditions. The total dissolved solid load of the samples was kept below 2 ppm for efficient analyte ionization during ICP-MS analysis. Dissolved samples were analyzed using an Agilent 7500cs (Agilent Technologies, Santa Clara, CA) quadrupole inductively coupled mass spectrometer equipped with an octopole reaction cell. A precleaned quartz sample introduction system, along with platinum extraction cones and a 100 μL nebulizer, was used to minimize blanks. The ICP-MS instrument was operated under hot plasma conditions (1500W RF), and sensitivity was optimized prior to each set of analyses. The ORC cell was optimized to knock out plasma- and matrix-based interference on analyte masses. External calibration using a multielement ICP standard (high purity standard) coupled with indium (In) standard addition was performed for accurate concentration determination. The reproducibility error for Cr, Mn, Fe, Co, Ni, and Zn on NIST SRM (1643e) was determined to be <3%.

DNA Binding Determined by Fluorescence Anisotropy. The Alexa-fluor 488-labeled promoter from the *fxbA* gene was used for all DNA binding experiments. The promoter sequences were 5′-Alex488 ATA CCG GCA TGC TAT CAA AGG TAA GGC TTA CCA ATG TGG GGC TCG TTG-3′ (forward) and 5′-CAA CGA GCC CCA CAT TGG TAA GCC TTA CCT TTG ATA GCA TGC CGG TAT-3′ (reverse). DNA was purchased as single strands (Integrated DNA Technologies Coralville, IA), and duplexes were generated by mixing equimolar amounts of forward and reverse strands, heating the mixture to 95 °C for 5 min, and slowly cooling the mixture to room temperature. Duplex formation was confirmed by migration on a 7% polyacrylamide gel, and the concentration was determined by the absorbance at 260 nm.

Fluorescence anisotropy experiments were performed using a Horiba Jobin (Edison, NJ) Yvon Fluoromax-4 spectrofluorometer with polarizers in the L-format. Measurements were taken at 25 °C using an excitation wavelength of 491 nm and an emission wavelength of 515 nm with 5 nm slit widths and an integration time of 10 s. Experiments were performed in one of two ways, by titrating metal into a solution containing DNA promoter (15 nM) and IdeR (750 nM) or by titrating metallated IdeR into a solution containing DNA promoter, in 10 mM MES (pH 6.8), containing 100 mM NaCl, 60 μg/mL BSA, 10 μg/mL poly(dI-dC) nucleotide, 5 mM $MgCl_2$, and 2 mM NAC. The steady state fluorescence anisotropy, *r*, at a given metal concentration, was calculated as

$$r = \frac{I_{\text{VV}} - GI_{\text{VH}}}{I_{\text{VV}} + 2GI_{\text{VH}}} \quad (2)$$

where I_{VV} is the fluorescence intensity with excitation and emission polarization in the vertical position, I_{VH} is the fluorescence intensity with excitation polarization in the vertical position and emission polarization in the horizontal position, and *G* is the ratio of the sensitivity of the detection system for vertically and horizontally polarized light. Each *r* value was normalized to the maximal change in *r* and plotted against the concentration of added divalent metal.

Analytical Ultracentrifugation (AUC). Sedimentation velocity experiments were performed using a Beckman Coulter (Brea, CA) XL-I analytical ultracentrifuge. The samples were run in buffer containing 10 mM MES, 100 mM NaCl, and 2 mM NAC (pH 6.8) at 20 °C, and metal was added to the appropriate concentration in the same buffer. Centrifugation cells were soaked in 50 mM EDTA overnight and rinsed thoroughly with Chelex-100-treated Nanopure water until they showed no absorption in the 220−350 nm range, indicating effective removal of the EDTA. The data were collected at 55000 rpm using absorbance optics and were scanned at either 230 or 280 nm depending on the protein concentration. Concentrations were from 0.1 to 0.9 OD unit, corresponding to values from 5.4 to 50 μM, respectively, for both the wild type.

dx.doi.org/10.1021/bi301608p | *Biochemistry* 2013, 52, 1927−1938

Ultrascan II was used for data analysis.[25] The partial specific volume was calculated to be 0.7399 mL/g based on protein sequence. The SOMO Bead modeling module in Ultrascan II was used to calculate theoretical hydrodynamic properties for monomeric and dimeric IdeR using PDB entry 1U8R.[26] Missing residues from the flexible linker in the crystal structure were automatically built using the approximate method in the module options. The monomer parameters were calculated using one monomer from the dimer crystal structure.

Data Analysis and Model Fitting. All data fitting, including calculation of 95% confidence intervals, was conducted with nonlinear regression using GraphPad (San Diego, CA) Prism version 5.03. The data were fit to four binding models.

(I) A single class of independent binding sites

$$r = \frac{n[\mathrm{x}]}{K_\mathrm{D} + [\mathrm{x}]} \tag{3}$$

where [x] is the free ligand concentration, n is the number of sites, and K_D is the dissociation constant.

(II) Multiple classes of independent binding sites

$$r = \frac{n[\mathrm{x}]}{K_n + [\mathrm{x}]} + \frac{m[\mathrm{x}]}{K_m + [\mathrm{x}]} \tag{4}$$

where n and m are the number of sites with invariant affinity for the two independent classes of sites, K_n is the dissociation constant of the n class of sites, and K_m is the dissociation constant of the m class of sites.

(III) Stoichiometric binding of 2 equiv of ligand

$$r = \frac{2[\mathrm{x}]^2 + K_2[\mathrm{x}]}{[\mathrm{x}]^2 + K_2[\mathrm{x}] + K_1K_2} \tag{5}$$

where K_1 is the dissociation constant of the first equivalent and K_2 is the dissociation constant of the second equivalent.

(IV) Phenomenological cooperative binding model

$$r = \frac{n[\mathrm{x}]^h}{K_\mathrm{D}{}^h + [\mathrm{x}]^h} \tag{6}$$

where n is the number of sites, K_D is the dissociation constant, and h is the Hill coefficient. Comparison of fits between different binding models was conducted using an F-test ($p < 0.05$) when comparing nested binding models (I–III) or an Akaike's Information Criteria (AICc) when comparing non-nested binding models (I–III vs IV).

Zn(II) Competition Metal Binding Assay. 4-(2-Pyridylazo)resorcinol (PAR) was used in a competition assay with IdeR.[27,28] PAR (200 μM) was mixed with 10 μM Zn(II) (ICP-MS standard grade), and the absorbance spectrum was recorded from 450 to 700 nm and blanked against a solution of 200 μM PAR. The experiment was repeated with increasing concentrations of IdeR until the absorbance of the PAR at 500 nm was reduced to approximately zero. With each addition of IdeR, the concentration of Zn(II) bound to PAR was determined from a standard curve of 200 μM PAR with known concentrations of Zn(II). The binding affinity of IdeR for Zn(II) was calculated according to the method of Walker and Imperiali[28] using only the absorbance values in the range of 20–80% of the initial PAR_2–Zn(II) absorbance.

RESULTS

Equilibrium Metal Binding by IdeR. The stoichiometry and binding affinity of IdeR for several divalent transition metal ions were obtained from equilibrium dialysis experiments. The buffer included 10 mM MES buffer, which has weak metal binding properties, 100 mM NaCl as a supporting electrolyte to reduce Donnan effects, and 2 mM *N*-acetyl-L-cysteine (NAC) as a reducing agent. The IdeR concentration was maintained at 30 μM, which should yield roughly 90% dimer in the absence of divalent metal based on the dimer dissociation constant reported previously.[29] The time to reach equilibrium for Ni(II) was established to be 18 h based on the absence of a change in the free metal concentration with time (data not shown). The same time was used for all metals.

Figure 2 plots the fraction of metal bound per IdeR monomer as a function of free metal concentration for the nitrate salts of Ni(II), Zn(II), Fe(II), and Mn(II). IdeR bound approximately 2 equiv of Ni(II), Zn(II), and Fe(II) and <1 equiv of Mn(II). Apparent binding parameters for each metal were obtained from fitting the data to specific binding isotherms, as described in Materials and Methods. As shown in Table 1, Mn(II) was best fit to a single class of independent sites, Fe(II) and Zn(II) were best fit to independent binding of metal into two sites, and Ni(II) was best fit to the phenomenological cooperative binding model. The K_D values obtained for Ni(II) binding were similar to values reported in previous studies.[29] The K_D values for the two Zn(II) and Fe(II) sites differed by ~70- and 25-fold, respectively. Regardless of the binding model, the order of relative binding affinity was determined to be as follows: Zn(II) (first equivalent) > Fe(II) (first equivalent) > Mn(II) ≫ Ni(II) > Fe(II) (second equivalent) > Zn(II) (second equivalent). The data demonstrate that binding of Fe(II) and Zn(II) by IdeR is thermodynamically different than that of other divalent transition metals.

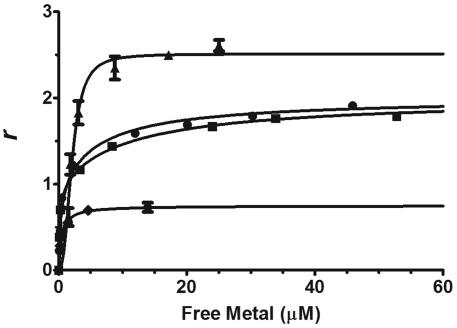

Figure 2. Equilibrium metal binding by IdeR. Plot of fraction bound (r) vs free metal concentration for IdeR. Solid lines represent the best fit of the data to eq 3, 4, 5, or 6, as described in Materials and Methods. The IdeR concentration was 30 μM in each experiment: Ni(II) (▲), Fe(II) (●), Zn(II) (■), and Mn(II) (◆). Data points (error bars) represent the average (standard deviation) of at least three independent measurements.

Binding of Fe(II) and Zn(II) by IdeR Mutants. IdeR contains two well-characterized metal binding sites. Previous work with DtxR, IdeR's closest homologue, established that Ala mutations of C102 and M10 in site II resulted in an inactive repressor whereas Ala mutations of E79 and H83 in site I reduced but did not abolish repressor activity.[18,30] We used these mutations to associate the thermodynamic binding "sites"

Table 1. Apparent Equilibrium Binding Parameters for IdeR Binding Various Divalent Metal Species

metal ion	K_D (μM)[a]	equiv of metal bound[a]	Hill coefficient[a]	binding isotherm[b]
Ni(II)	2.18 (1.89, 2.47)	2.60 (2.45, 2.75)	2.25 (1.39, 3.11)	cooperative
Fe(II)	0.28 (0.17, 0.39)	1	NA	stoichiometric[c]
	6.65 (3.4, 9.88)	1	NA	
Mn(II)	0.56 (0.01, 0.63)	0.75 (0.71, 0.79)	NA	single class
Zn(II)	0.17 (0.12, 0.22)	1	NA	stoichiometric[c]
	11.17 (8.63, 13.71)	1	NA	

[a]Values in parentheses represent the 95% confidence interval. [b]Fits were compared using Akaike's criterion (AICc), and models displaying >90% probability were selected. [c]The data fit to stoichiometric binding with 2 equiv (eq 5 in Materials and Methods).

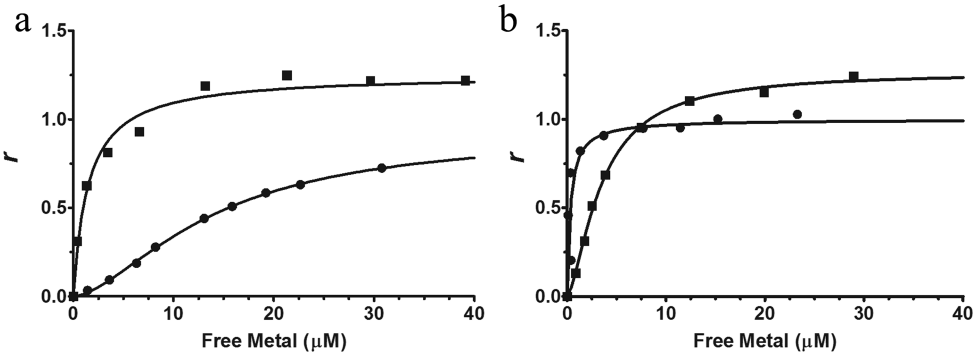

Figure 3. Binding of Fe(II) and Zn(II) to IdeR metal site mutants. (a) Plot of fraction bound (r) vs free metal concentration for E83A. (b) Plot of fraction bound (r) vs free metal concentration for C102A. Data points represent a single measurement. Solid lines represent the best fit of the data to eq 3, 4, 5, or 6, as described in Materials and Methods. The IdeR concentration was 30 μM in each experiment: Zn(II) (■) and Fe(II) (●).

with the physical binding sites for both Fe(II) and Zn(II). Previous studies determined that none of the mutations significantly change the protein secondary structure[10] but can alter some of the loose tertiary structure present in the apoprotein.[31]

Figure 3a compares the equilibrium binding of Fe(II) and Zn(II) by the E83A site I mutant. Quantitative binding parameters for these data are listed in Table 2. As seen in the figure, Fe(II) binding was severely perturbed in the E83A site I mutant whereas this mutant still showed high-affinity binding of 1 equiv of Zn(II). By comparison, the C102A site II mutant showed high-affinity binding for 1 equiv of Fe(II) (Figure 3b). C102A showed binding of 1 equiv of Zn(II), although with reduced affinity compared to that of the wild type (Table 2). Taken together, the data strongly associate the high-affinity Fe(II) binding site with site I. This suggests that the high-affinity Zn(II) binding site should be assigned to the physical site II, but because both mutants alter Zn(II) binding to approximately the same extent, this assignment is more tentative than the Fe(II) binding results.

Table 2. Apparent Equilibrium Binding Parameters for IdeR Site Mutants with Fe(II) and Zn(II)

mutant	metal	K_D (μM)[a]	equiv of metal bound[a]
E83A	Fe(II)	13.93 (12.40, 15.46)	0.92 (0.85, 0.99)
E83A	Zn(II)	1.48 (0.95, 2.02)	1.25 (1.18, 1.33)
C102A	Fe(II)	0.33 (0.01, 0.66)	1.00 (0.82, 1.18)
C102A	Zn(II)	3.47 (3.07, 3.87)	1.27 (1.20, 1.33)

[a]Values in parentheses represent the 95% confidence interval.

Competition with PAR Reveals IdeR Binds Zn(II) Very Tightly. The apparent Zn(II) affinity obtained in the equilibrium dialysis experiments was weaker than that reported for other Zn(II) binding proteins, bringing into question the physiological relevance of this binding. Therefore, Zn(II) binding by IdeR was measured using the competition metal binding assay described by Jefferson et al.[27] and Walkup and Imperiali.[28] This assay is based on competition with 4-(2-pyridylazo)resorcinol (PAR), monitoring changes in the level of the PAR_2–Zn(II) complex in solution upon addition of IdeR. Excess PAR was used to ensure that >99% of the PAR–Zn complex was PAR_2–Zn. Titrating apo-IdeR into the solution containing the PAR_2–Zn(II) complex reduced the absorbance of the PAR_2–Zn(II) complex. As shown in Figure 4a, the addition of increasing concentrations of IdeR reduced the absorbance of PAR to the noise level, yielding a dissociation constant of 3.6×10^{-11} M with an apparent stoichiometry of one Zn(II) per IdeR monomer.

The competition binding assay was used to determine whether NAC present in the equilibrium dialysis buffer might contribute to the discrepancy between the dialysis and competition binding results. Under the conditions used in these assays (pH 6.8), the binding stoichiometry is expected to be NAC_2–Zn(II).[32] Titrating NAC to the concentration used in the equilibrium dialysis experiments (2 mM) reduced the 500 nm absorbance of the PAR_2–Zn(II) complex, similar to that observed upon titration of IdeR (not shown). Given that NAC was present in a 70-fold excess compared to IdeR in the equilibrium dialysis experiment, coordination of Zn(II) by NAC could effectively compete with binding of Zn(II) by IdeR. The analysis of our equilibrium data would not capture these additional equilibria, so the binding parameters reported in Tables 1–3 should be considered as upper limits.

Zn(II) Binding Enhances Dimer Formation More Effectively Than Fe(II). The effect of Fe(II) and Zn(II) binding on the dimerization of IdeR was investigated using analytical ultracentrifugation. Figure 5 shows the $G(s)$ plot obtained from a series of sedimentation velocity experiments

dx.doi.org/10.1021/bi301608p | Biochemistry 2013, 52, 1927–1938

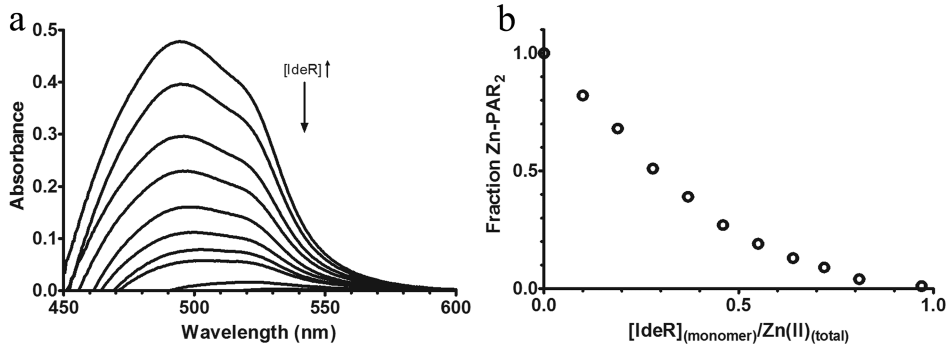

Figure 4. Titration of the PAR_2−Zn(II) complex with increasing concentrations of IdeR and Zn(II) competition binding assay. (a) Absorbance spectra of 200 μM PAR and 10 μM Zn(II) with increasing concentrations of IdeR blanked against 200 μM PAR without Zn(II) present. (b) Plot of the fraction of the Zn(II)−PAR complex vs IdeR monomer:Zn(II) ratio. A solution of 200 μM PAR containing 10 μM Zn(II) was titrated with wild-type IdeR, and the decrease in absorbance of PAR was used to determine the amount of Zn(II) bound to IdeR as described in Materials and Methods.

Table 3. Equilibrium Binding Parameters for IdeR and Fe(II) with Zn(II) Present

titrating metal ion	K_D (μM)[c]	equiv of metal bound[c]
Fe(II)[a]	0.89 (0.31, 1.5)	1.12 (1.00, 1.24)
Zn(II)[b]	1.19 (0.31, 2.07)	1.02 (0.93, 1.12)

[a]Titration was performed in the presence of 1 equiv of Zn(II). The best model fit changed to a single class of binding sites. [b]Titration was performed in the presence of a 3-fold excess of Fe(II). The best model fit changed to a single class of binding sites. [c]Values in parentheses represent the 95% confidence interval.

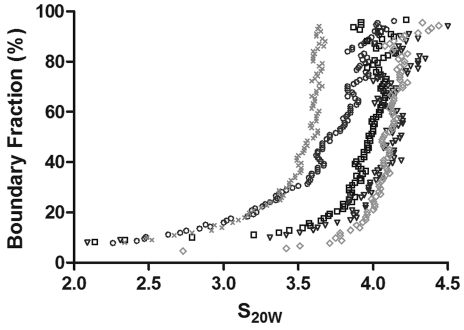

Figure 5. Metal-dependent *s* value distributions. Plot of sedimentation coefficients (*s*) vs boundary fraction in the absence or presence of metal. The IdeR concentration was 15 μM in each experiment: apo (gray ×), 1× Zn(II) (□), 1× Zn(II) and 1× Fe(II) (▽), 1× Fe(II) (○), and 10× Fe(II) (gray ◇).

performed with IdeR. Apo-IdeR exhibited an apparent value of 3.6 S. This corresponds to 24% monomer, calculated using a bead model[33,34] for a monomer of IdeR that assumed the monomer retains the same structure as that observed in the dimer.[26] This simple model almost certainly underestimates the true hydrodynamic ratio because of the partial unfolding of the protein structure in the absence of metal.[35] In the presence of an excess of Fe(II), the value increased to 4.1 S, which is consistent with 100% dimer formation based on the hydrodynamic properties calculated using the bead model. By comparison with the narrow distribution induced by excess Fe(II), a broad distribution of *s* values ranging from 3.6 to 4.1 S was obtained in the presence of a single stoichiometric equivalent of Fe(II). This suggests that the extent of dimer formation is significantly reduced upon binding 1 equiv of Fe(II). In contrast to the Fe(II) results, however, 1 equiv of Zn(II) yielded a single, apparent *s* value of 4.0 S, corresponding to approximately 90% dimer formation. The crystal structures of DtxR and IdeR display relatively small root-mean-square deviations between different metal-bound forms,[17,36,37] suggesting that conformational changes are not the source of the different *s* values obtained for Fe(II) and Zn(II). Finally, addition of 1 equiv each of Fe(II) and Zn(II) yielded an *s* value similar to that of Zn(II) alone or of excess Fe(II). Thus, 1 equiv of Zn(II) is more effective at inducing dimer formation than 1 equiv of Fe(II), and addition of Fe(II) and Zn(II) together yields a species having hydrodynamic properties similar to those of the Fe(II)-saturated protein.

Does Zn(II) Binding Enhance Fe(II) Binding by IdeR?

The similarity in binding of Fe(II) and Zn(II), coupled with the physically and thermodynamically unique Fe(II) and Zn(II) binding sites, raised the possibility that IdeR is a mixed-metal repressor, binding Fe(II) in site I and Zn(II) in site II. Several metal-activated repressors contain both "structural" and "functional" metal binding sites.[16] The possibility that site II serves as a structural site was investigated by measuring the binding of Fe(II) by IdeR that was pre-equilibrated with 1 equiv of Zn(II). In these experiments, metal concentrations were determined using inductively coupled plasma mass spectrometry (ICP-MS) to generate simultaneous binding curves for the two metal species present. Control ICP-MS experiments performed with Fe(II) alone showed an affinity for Fe(II) binding slightly higher than that determined using terpy (not shown), probably reflecting the different sample workup and the absence of competition binding between IdeR and terpy. Figure 6a shows simultaneous Zn(II) and Fe(II) metal binding curves obtained at increasing Fe(II) concentrations in the presence of 1 molar equiv of Zn(II). The data show a slight reduction in the amount of bound Zn(II) as the level of Fe(II) is increased but reached 1 equiv of both metals bound at high Fe(II) concentrations. Figure 6b shows a simultaneous binding curve for both metals obtained by pre-equilibrating IdeR with excess Fe(II) and then titrating with Zn(II). Zn(II) displaced 1 equiv of bound Fe(II), with the end point again showing essentially 1 equiv of both metals bound.

Thermodynamic parameters obtained from fitting these data are listed in Table 3, which shows that pre-equilibration with Zn(II) did not significantly change the Fe(II) binding affinity compared to the affinity in the absence of Zn(II). On the other hand, Fe(II) slightly reduced the affinity for Zn(II). The data support a model in which IdeR binds 1 equiv of Fe(II) and

dx.doi.org/10.1021/bi301608p | *Biochemistry* 2013, 52, 1927−1938

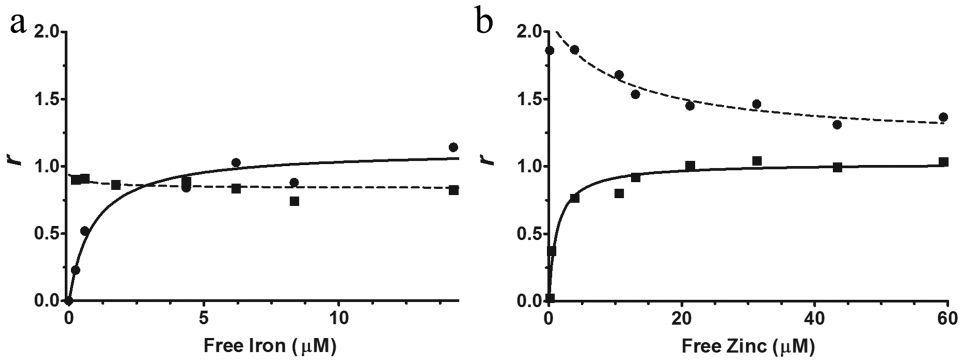

Figure 6. Binding of Fe(II) to IdeR in the presence of Zn(II). (a) Plot of fraction bound (r) vs free Fe(II) concentration in the presence of 1× Zn(II). (b) Plot of fraction bound (r) vs free Zn(II) concentration in the presence of 3× Fe(II). Solid lines represent the best fit of the data to eq 3, 4, 5, or 6, as described in Materials and Methods. The dashed lines are trend lines for indicating changes in the stoichiometric amount of pre-equilibrated secondary metal bound as a function of free metal concentration. The IdeR concentration was 30 μM in each experiment: Fe(II) (●) and Zn(II) (■).

Zn(II) simultaneously, but Zn(II) binding does not enhance Fe(II) binding.

Metal Activation of Promoter Binding. Numerous studies have shown that Fe(II) is the physiological ligand for activating IdeR and its homologue, DtxR, for promoter binding.[7,38] Metal activation of promoter binding was investigated using a coupled metal−DNA binding assay similar to that described by Chou et al.,[12] in which divalent metal is titrated into a solution containing apo-IdeR and dye-labeled duplex DNA corresponding to the *fxbA* promoter site. Figure 7

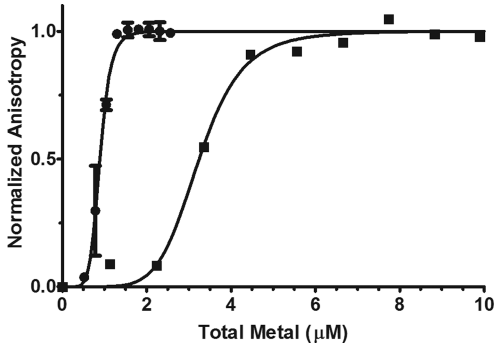

Figure 7. Metal activation of *fxbA* promoter binding. Change in the normalized fluorescence anisotropy of Alexa-fluor 488-labeled *fxbA* promoter DNA in the presence of IdeR as a function of total metal added. Fe(II) or Zn(II) was titrated into buffer containing IdeR (750 nM), *fxbA* promoter (15 nM) in 10 mM MES buffer (pH 6.8) containing NaCl, BSA, and poly(dI-dC) (see Materials and Methods). Data points (error bars) represent the average (standard deviation) of at least three independent determinations. The solid lines represent the curves fit best to eq 6.

and Table 4 show that both Fe(II) and Zn(II) alone were able to induce promoter binding in IdeR, with Fe(II) activating promoter binding at significantly lower metal concentrations and with higher cooperativity than Zn(II). The observed binding parameters reported here indicate slightly tighter binding than what had been reported previously.[12] This difference can be attributed to the buffer used (the choice of buffer was previously shown to have a substantial impact on metal binding by IdeR[29]) and the use of 100 mM rather than 10 mM NaCl [promoter binding by IdeR exhibits a strong dependence on salt concentration (unpublished observations)].

Table 4. Apparent Binding Parameters for Metal-Induced Promoter Binding

titrated metal ion	K_D (μM)[a]	Hill coefficient[a]	secondary metal[b]
Fe(II)	0.89 (0.86, 0.93)	7.1 (5.4, 8.7)	–
Zn(II)	3.2 (3.1, 3.4)	6.3 (4.4, 8.3)	–
Fe(II)	0.29 (0.27, 0.31)	3.4 (2.7, 4.1)	1× Zn(II)
Fe(II)	0.030 (0.028, 0.032)	2.9 (2.2, 3.5)	3× Zn(II)

[a]Values in parentheses represent the 95% confidence interval. [b]IdeR was pre-equilibrated with this metal for 1 h before titration with Fe(II).

The apparent affinity for promoter binding in this assay corresponds to an Fe(II) concentration at which roughly 95% of the IdeR contains 1 equiv of bound Fe(II). The promoter binding assay was modified to investigate whether IdeR with 1 equiv of bound Fe(II) was active for promoter binding by titrating IdeR and Fe(II) at a fixed stoichiometric ratio. No promoter binding was observed under these conditions, nor was promoter binding activity detected upon cotitration of IdeR with 1 equiv of Zn(II) (not shown). However, when IdeR was saturated with either Fe(II) or Zn(II) and titrated into a solution containing the *fxbA* promoter under metal saturating conditions, strong binding was observed (Figure 8), with Fe(II)-loaded IdeR exhibiting a slightly higher affinity than

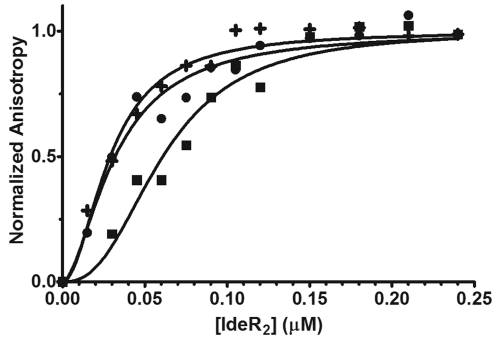

Figure 8. IdeR promoter binding. IdeR in presence of Fe(II) (●), Zn(II) (■), or a combination of Fe(II) and Zn(II) (+) was titrated into a solution containing *fxbA* promoter also containing divalent metal as described in Materials and Methods. Normalized anisotropy plotted vs total IdeR dimer concentration. The solid lines represent the curves fit best to eq 6 as described in Materials and Methods.

dx.doi.org/10.1021/bi301608p | *Biochemistry* 2013, 52, 1927−1938

Zn(II)-loaded IdeR (Table 5). These binding processes were also characterized by a cooperative binding model, with a Hill coefficient of 2.

Table 5. Apparent Binding Parameters for Promoter Binding

metal ion(s)	K_D (μM)[a]	Hill coefficient[a]
Fe(II)	0.032 (0.026, 0.038)	1.7 (1.3, 2.2)
Zn(II)	0.061 (0.053, 0.069)	2.5 (1.8, 3.3)
Fe(II) and Zn(II)	0.029 (0.025, 0.033)	1.9 (1.5, 2.3)

[a]Values in parentheses represent the 95% confidence interval.

Zn(II) Enhances Fe(II)-Induced Promoter Binding. We wondered whether pre-equilibration with Zn(II) would affect the apparent affinity for Fe(II)-induced promoter binding. In this experiment, IdeR was pre-equilibrated with 1 equiv of Zn(II) in the presence of the *fxbA* promoter and promoter binding induced by titration with Fe(II). Under these conditions (Figure 9a), full promoter binding required less Fe(II) than when Fe(II) was titrated alone. The sensitivity to Fe(II) concentration was further enhanced in the presence of a slight excess of Zn(II) (Figure 9b). Quantitatively, pre-equilibration with Zn(II) resulted in an ~30-fold reduction in the Fe(II) concentration necessary to induce binding to the *fxbA* promoter compared to that required for Fe(II) alone (Table 4). The cooperativity of promoter binding was decreased by the presence of Zn(II), perhaps reflecting the increased amount of dimeric IdeR induced by addition of Zn(II). It is important to point out that adding Zn(II) alone did not change the observed anisotropy and that the total anisotropy change induced by Fe(II) at either Zn(II) concentration was similar to that induced by Fe(II) alone. These same studies were repeated with similar ratios of Mn(II) rather than Zn(II), but this resulted in more modest enhancement of Fe(II) sensitivity [~2× and ~4×, respectively (not shown)]. This result argues against a generalized metal concentration effect as the basis for the enhancement in promoter activity and suggests that this effect is more specific to the Zn(II)-bound form of IdeR.

Finally, we pre-equilibrated IdeR with 1 equiv of both Fe(II) and Zn(II) and titrated that into a solution of the *fxbA* promoter while maintaining the fixed metal:IdeR ratio. As shown in Figure 8, this resulted in high-affinity promoter binding, with the affinity being equal to that of iron-saturated IdeR.

DISCUSSION

IdeR and its homologues function as Fe(II) sensors in bacteria by binding iron and regulating the expression of numerous genes. Although Fe(II) was established to be the physiological metal ion in IdeR,[8] a detailed study of Fe(II) binding and activation for promoter binding has not yet appeared. All previously published studies of binding of Fe(II) by IdeR or DtxR fall into one of three categories: (1) in vivo assays in which the nature of the metal-bound protein was not investigated,[18] (2) indirect binding assays that did not quantify the stoichiometry of bound metal,[12] or (3) binding assays in which the stoichiometry was quantified only under saturating conditions.[11] In this study, Fe(II) binding was investigated under conditions where a complete binding profile, e.g., binding energetics and stoichiometry, could be determined and where this binding could be directly related to functional activity. The results of this study allow us to extend the general model for metal activation in IdeR and, by extension, other two-domain members of the DtxR family of iron sensor proteins. This model is presented in Figure 10. Evidence in support of this model is discussed below.

State A: Apo-IdeR. We and others have established that IdeR and DtxR are predominantly monomeric and are weakly folded in solution in the absence of divalent metal, e.g., state A in Figure 10.[29,31,35] Studies have shown that IdeR has no promoter binding activity when no metal is present.[7] The sedimentation velocity data presented in Figure 5 are consistent with this, establishing that apo-IdeR is better characterized as a monomer than a dimer.

State B: Binding the First Equivalent of Metal. *IdeR Contains Two Thermodynamically Distinct Metal Binding Sites.* The equilibrium dialysis results presented in Figure 2 show that IdeR binds Fe(II) in two thermodynamically distinct steps with dissociation constants differing by ~20-fold. The thermodynamic processes were associated with specific physical binding sites through the use of binding site mutants (Figure 3), establishing site I as the high-affinity and site II as the low-affinity Fe(II) binding site. Interestingly, Zn(II) was the only

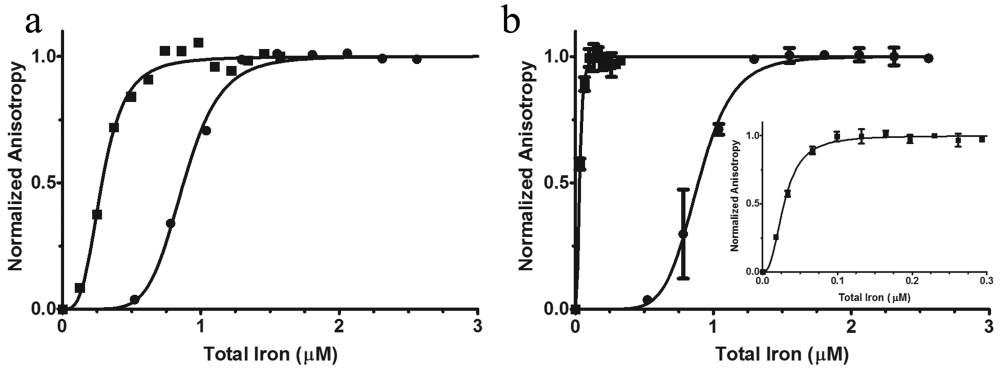

Figure 9. Zn(II) enhanced Fe(II)-activated promoter binding. (a) Fe(II)-dependent promoter binding with 1× Zn(II) present. Fe(II) was titrated into a buffer containing 1 molar equiv of Zn(II) (■) as described in Materials and Methods. Normalized anisotropy plotted vs total Fe(II) added. Fe(II) (●) data were recorded in the absence of a secondary metal. (b) Fe(II) was titrated into a buffer containing 3 molar equiv of Zn(II) (■) as described in Materials and Methods. Normalized anisotropy plotted vs total Fe(II) added. Fe(II) (●) data were recorded in the absence of secondary metal. The inset shows Fe(II)-dependent titration of IdeR-*fxbA* with 3× Zn(II) present. Data points (error bars) represent the average (standard deviation) of at least three independent determinations. The solid lines represent the curves fit best to eq 6 (Materials and Methods).

dx.doi.org/10.1021/bi301608p | *Biochemistry* 2013, 52, 1927−1938

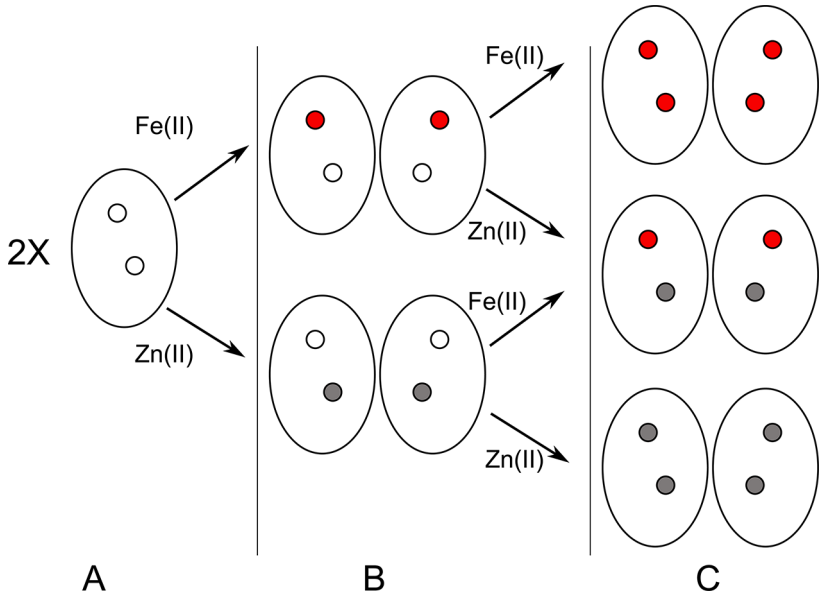

Figure 10. Extended model for metal activation of IdeR. The functional site is depicted as the upper site, and the structural site is depicted as the lower site. The apoprotein can bind either Fe(II) in the functional site or Zn(II) in the structural site. Binding of Fe(II) to the functional site leads directly to promoter binding, although the promoter binding affinity is low. Additional Fe(II) can then be bound by the structural site, but without the enhancement of promoter binding affinity. Similarly, Zn(II) can be bound first in the structural site and subsequently in the functional site, leading to weak DNA binding. The highest promoter binding activity is achieved with Fe(II) bound in the functional site and Zn(II) bound in the structural site.

other metal that exhibited a similar binding profile, with 1 equiv of metal bound in two thermodynamically distinct events. The two Zn(II) binding events had apparent dissociation constants that differed by ~70-fold, with the first equivalent of Zn(II) (K_D ~ 170 nM) binding with a higher affinity than the first equivalent of Fe(II). When Zn(II) binding was re-examined in a competitive binding assay (Figure 4), we discovered that IdeR binds Zn(II) with extremely high affinity, on par with that of other, well-established Zn(II)-binding proteins.[39] The reasons for the discrepancy between the equilibrium dialysis and competitive binding assays are most likely related to avid binding of Zn(II) by NAC present at millimolar concentrations in the equilibrium dialysis buffer. A similar observation has been reported for SmtB, which was reported to bind Zn(II) in the micromolar range by equilibrium dialysis[40] but was subsequently found to bind significantly tighter when re-examined in a competitive binding assay.[39] In this case, the equilibrium dialysis experiments were performed in the presence of nitrilotriacetate (NTA), a Zn(II) chelating agent, whereas the competition experiments were not.

Metal binding by IdeR mutants clearly established site I as the high-affinity Fe(II) binding site, but the data were less conclusive for Zn(II). However, the mixed metal binding studies established that the first equivalent of bound Fe(II) does not compete with Zn(II) binding, and that addition of Zn(II) to Fe(II)-saturated IdeR released only 1 equiv of Fe(II). Together, these studies suggested that the high-affinity sites were different for Zn(II) and Fe(II), and therefore, we assigned the high-affinity Zn(II) site to site II.

Binding One Equivalent of Metal Increases the Extent of Dimer Formation. Several studies have associated a disordered to ordered structural transition upon metal binding in IdeR and its closest homologue, DtxR, with a concurrent increase in the level of dimer formation.[31,35,41] The sedimentation velocity data presented in Figure 5 provide further refinement of these earlier results. Specifically, apo-IdeR is characterized as a single species with a sedimentation coefficient corresponding approximately to that expected for a monomer of IdeR. Addition of Fe(II) yielded a distribution of $G(s)$ values, suggesting either a broad distribution of aggregation states or a monomer−dimer equilibrium with dissociation rates on the same order of magnitude as those from the sedimentation velocity experiment.[42] On the other hand, binding 1 equiv of Zn(II) resulted in essentially complete dimer formation, with an s value similar to that obtained in the presence of a saturating amount of Fe(II). These results suggest that binding 1 equiv of Zn(II) may serve to preorganize IdeR for binding a second equivalent of metal.

State C: Two Equivalents of Divalent Metal Activates IdeR for Promoter Binding. IdeR is activated for promoter binding when 2 equiv of metal is bound, a finding that is consistent with all previous quantitative studies of IdeR and DtxR. In agreement with data presented by Chou et al.,[12] we showed that Fe(II) was the strongest activator of promoter binding in a coupled metal-DNA binding assay (Figure 7) compared to other divalent transition metal ions. Given the high level of intracellular Fe(II) compared with the levels of other divalent metals,[43] this suggests that IdeR would be most responsive to changes in Fe(II) concentration and provides a straightforward basis for metal selectivity in IdeR, namely, that Fe(II)-activated IdeR has the highest affinity for DNA binding.

However, the story became more interesting when IdeR was saturated with metal and titrated into a solution containing the *fxbA* promoter. Under these conditions, we observed similar promoter binding affinities for Fe(II)- and Zn(II)-activated IdeR (32 and 61 nM, respectively). Thus, metal loading, rather than the specific bound metal, appears to be the critical factor in DNA binding. Other evidence for this idea comes from the observation that crystal structures of IdeR or DtxR saturated

dx.doi.org/10.1021/bi301608p | *Biochemistry* 2013, 52, 1927−1938

with various divalent transition metals all have essentially the same structures.

We then wondered whether a mixture of Zn(II) and Fe(II) could activate IdeR, given that IdeR has a very high-affinity site for Zn(II). Indeed, the data presented in Figures 8 and 9 show that Zn(II) acts synergistically with Fe(II) to enhance the promoter binding activity of IdeR, presumably by increasing the amount of dimer present. Importantly, Figure 6 clearly shows that IdeR can bind 1 equiv each of Zn(II) and Fe(II) and that Zn(II) binding does not significantly alter high-affinity Fe(II) binding. These experiments suggest that Zn(II) co-activation of IdeR produces a better regulatory switch than Fe(II) alone, because the Zn−IdeR complex would be better able to transmit small changes in iron concentration into effective gene regulation. By comparison, activation of IdeR by Fe(II) alone would only be effective at significantly higher Fe(II) concentrations and would require larger fluctuations of Fe(II) concentrations.

There are other lines of evidence that support the validity of this Zn(II) co-activation model. First, the coordinating residues in the structural and regulatory sites of IdeR are consistent with a preference for Zn(II) and Fe(II), respectively. Dokmanić et al.[44] surveyed ∼10000 metal-bound proteins present in the PDB and found that, of the more than 1000 proteins with Zn(II) bound, the most common coordinating residues are Cys (∼47%) and His (∼33%). By comparison, the IdeR structural site contains two sulfur ligands (C102 and M10) and one His ligand (H106). Furthermore, of the ∼550 Fe(II) binding proteins in the PDB, the most common coordinating residues for Fe(II) are His (∼65%) and Glu (∼10%). Again, this coordination chemistry is consistent with the regulatory site of IdeR but not with the structural site.

Second, many metal-responsive repressors contain both structural and functional metal binding sites.[16] For example, CadC contains a nonregulatory Zn(II)/Co(II) site with the Zn(II) or Co(II) coordinated by His and carboxylate residues.[45] Alternatively, PerR, a oxidative stress repressor, and Fur, which is the other bacterial Fe(II) regulator, both contain a structural Zn(II) site and an Fe(II) binding regulatory site.[46,47] In these proteins, Zn(II) is coordinated by four cysteine residues. Thus, we interpret the Zn(II) binding affinity to be within the limits of bioavailable zinc and to serve a structural role by promoting the amount of dimer present. We now refer to site II or the primary site of IdeR as the structural metal binding site and the Fe(II) binding site (site I or ancillary site) as the regulatory metal binding site.

One of the open questions regarding iron sensing by IdeR was how the relatively high concentrations of Fe(II) required to trigger promoter binding coupled with the relatively weak promoter binding induced by Fe(II) in vitro lead to effective in vivo gene regulation. Our results clearly demonstrate that Zn(II) costimulation translates the Fe(II) sensitivity of IdeR DNA binding into a concentration range that may be more relevant for the mammalian environment than if promoter binding were triggered by Fe(II) binding alone. Total intracellular Zn(II) concentrations range from 200 to 300 μM in bacteria,[48] although free Zn(II) levels are substantially lower than that, and Zn(II) is the primary metal present in mast cells.[49] Therefore, picomolar binding of Zn(II) by IdeR and the resulting enhanced sensitivity to Fe(II) fluctuations could be biologically relevant. This study shows that IdeR has three possible fully metalated active states (Fe_2·IdeR, Zn_2·IdeR, and Zn·IdeR·Fe), yet we suggest that only two are relevant in vivo because the bioavailable Zn(II) concentration is only high enough to have a single Zn(II) bound at the high-affinity site. IdeR may have two levels of Fe(II) sensing, but the Zn(II) and Fe(II) state would provide an appropriate sensory range for Fe(II) levels in the bacterium. Within this model, we hypothesize that IdeR contains 1 equiv of bound Zn(II) as a structural metal (Zn·IdeR). At high levels of Fe(II), Zn·IdeR also contains 1 equiv of Fe(II) bound in the regulatory site, generating the promoter binding competent form (Zn·IdeR·Fe) and repressing expression of iron acquisition, uptake, and utilization genes. However, as Fe(II) levels drop, IdeR converts back to Zn·IdeR, derepressing expression of the IdeR regulon.

Interestingly, the picomolar Zn(II) apparent dissociation constant reported here is higher than that observed for other Zn(II) binding proteins. This suggests that IdeR could, under Zn(II)-depleted conditions, cycle between Zn·IdeR and apo-IdeR. This might allow for a different spectrum of promoter binding,[50] resulting in coordinate regulation of Fe(II) and Zn(II) in vivo. The IdeR regulon contains many ABC transporter proteins of unknown function,[4] some of which might be involved in Zn(II) uptake and transport. Indeed, the *M. tuberculosis* ESX-3 gene cluster, which is involved in optimizing uptake of zinc and iron for growth,[51] is jointly regulated by IdeR[5] and Zur[52] binding.

Fe(II) availability is very low in mammalian systems. Indeed, it is the bacterial response to low iron levels that triggers the virulence response in *M. tuberculosis*. Zn(II) concentrations are high in the mammalian host but are highly variable in soils where *M. tuberculosis* resides outside of mammalian hosts. We speculate that the ability to modulate IdeR activity using Fe(II) alone provides an evolutionary advantage to the bacterium because it could allow IdeR to regulate expression of Fe(II)-sensitive genes when the Zn(II) concentration is very low. Under these conditions, significantly larger amounts of Fe(II) are required to activate IdeR. Gold et al.[4] demonstrated that IdeR can also function as an activator of genes to upregulate production of bacterioferritin (and other iron storage proteins) to prevent oxidative stress caused by intracellular iron. Thus, the reduced sensitivity to Fe(II) concentration changes may allow IdeR to also regulate a different set of genes involved in iron storage or efflux. The in vivo concentration of other metals is often coregulated by different repressors having significantly different metal binding affinities.[53] It is interesting to speculate that IdeR may also afford similar regulation of iron, in both high and low concentration ranges, simply based on the presence of zinc.

AUTHOR INFORMATION

Corresponding Author

*E-mail: tlogan@fsu.edu. Phone: (850) 644-8979.

Author Contributions

B.S. and L.R.W. contributed equally to this work.

Funding

The work was supported by National Institutes of Health Grant 2R01 AI021628.

Notes

The authors declare no competing financial interest.

ACKNOWLEDGMENTS

We thank Dr. Pamela Twigg for careful review of the manuscript and many helpful discussions and Dr. Vincent Salters, Sambuddha Misra, and Afi Sachi-Kocher of Florida

State University and the National High Magnetic Field Laboratory for training on and access to the ICP mass spectrometer for metal concentration analysis. Molecular graphics and analyses were performed with the UCSF Chimera package made available at http://www.cgl.ucsf.edu/chimera/download.html. The analytical ultracentrifuge was purchased with support from the National Institutes of Health (1S10 RR022364).

■ ABBREVIATIONS

IdeR, iron-dependent regulator; DtxR, diphtheria toxin repressor; MES, 2-(*N*-morpholino)ethanesulfonic acid; TCEP, tris(2-carboxyethyl)phosphine; EDTA, ethylenediaminetetraacetic acid; DTT, dithiothreitol; NAC, *N*-acetyl-L-cysteine; terpy, 2,2′;6′,2″-terpyridine; BSA, bovine serum albumin; AICc, small-sample-size corrected Akaike information criterion; CadC, cadmium efflux system accessory protein; PerR, peroxide-responsive repressor; Fur, ferric uptake regulator; PAR, 4-(2-pyridylazo)resorcinol; PDB, Protein Data Bank.

■ REFERENCES

(1) CDC|TB|Data and Statistics. http://www.cdc.gov/tb/statistics/default.htm (accessed Nov 20, 2012).
(2) Litwin, C. M., and Calderwood, S. B. (1993) Role of iron in regulation of virulence genes. *Clin. Microbiol. Rev. 6*, 137−149.
(3) Ranjan, S., Yellaboina, S., and Ranjan, A. (2006) IdeR in *Mycobacteria*: From Target Recognition to Physiological Function. *Crit. Rev. Microbiol. 32*, 69−75.
(4) Gold, B., Rodriguez, G. M., Marras, S. A., Pentecost, M., and Smith, I. (2001) The *Mycobacterium tuberculosis* IdeR is a dual functional regulator that controls transcription of genes involved in iron acquisition, iron storage and survival in macrophages. *Mol. Microbiol. 42*, 851−865.
(5) Rodriguez, G. M., Voskuil, M. I., Gold, B., Schoolnik, G. K., and Smith, I. (2002) ideR, an essential gene in *Mycobacterium tuberculosis*: Role of IdeR in iron-dependent gene expression, iron metabolism, and oxidative stress response. *Infect. Immun. 70*, 3371−3381.
(6) Marcela Rodriguez, G., Gold, B., Gomez, M., Dussurget, O., and Smith, I. (1999) Identification and characterization of two divergently transcribed iron regulated genes in *Mycobacterium tuberculosis*. *Tubercle Lung Dis. 79*, 287−298.
(7) Schmitt, M. P., Predich, M., Doukhan, L., Smith, I., and Holmes, R. K. (1995) Characterization of an iron-dependent regulatory protein (IdeR) of *Mycobacterium tuberculosis* as a functional homolog of the diphtheria toxin repressor (DtxR) from *Corynebacterium diphtheriae*. *Infect. Immun. 63*, 4284−4289.
(8) Dussurget, O., Timm, J., Gomez, M., Gold, B., Yu, S., Sabol, S. Z., Holmes, R. K., Jacobs, W. R., and Smith, I. (1999) Transcriptional Control of the Iron-Responsive fxbA Gene by the Mycobacterial Regulator IdeR. *J. Bacteriol. 181*, 3402−3408.
(9) Hobson, R., McBride, A., Kempsell, K., and Dale, J. (2002) Use of an arrayed promoter-probe library for the identification of macrophage-regulated genes in *Mycobacterium tuberculosis*. *Microbiology 148*, 1571−1579.
(10) D'Aquino, J. A., Tetenbaum-Novatt, J., White, A., Berkovitch, F., and Ringe, D. (2005) Mechanism of metal ion activation of the diphtheria toxin repressor DtxR. *Proc. Natl. Acad. Sci. U.S.A. 102*, 18408−18413.
(11) Spiering, M. M., Ringe, D., Murphy, J. R., and Marletta, M. A. (2003) Metal stoichiometry and functional studies of the diphtheria toxin repressor. *Proc. Natl. Acad. Sci. U.S.A. 100*, 3808−3813.
(12) Chou, C. J., Wisedchaisri, G., Monfeli, R. R., Oram, D. M., Holmes, R. K., Hol, W. G. J., and Beeson, C. (2004) Functional Studies of the *Mycobacterium tuberculosis* Iron-dependent Regulator. *J. Biol. Chem. 279*, 53554−53561.
(13) Ma, Z., Gabriel, S. E., and Helmann, J. D. (2011) Sequential binding and sensing of Zn(II) by *Bacillus subtilis* Zur. *Nucleic Acids Res. 39*, 9130−9138.
(14) Reyes-Caballero, H., Lee, C. W., and Giedroc, D. P. (2011) *Mycobacterium tuberculosis* NmtR Harbors a Nickel Sensing Site with Parallels to *Escherichia coli* RcnR. *Biochemistry 50*, 7941−7952.
(15) Bellini, P., and Hemmings, A. M. (2006) In Vitro Characterization of a Bacterial Manganese Uptake Regulator of the Fur Superfamily. *Biochemistry 45*, 2686−2698.
(16) Ma, Z., Jacobsen, F. E., and Giedroc, D. P. (2009) Coordination Chemistry of Bacterial Metal Transport and Sensing. *Chem. Rev. 109*, 4644−4681.
(17) Qiu, X., Verlinde, C. L. M., Zhang, S., Schmitt, M. P., Holmes, R. K., and Hol, W. G. (1995) Three-dimensional structure of the diphtheria toxin repressor in complex with divalent cation co-repressors. *Structure 3*, 87−100.
(18) Ding, X., Zeng, H., Schiering, N., Ringe, D., and Murphy, J. R. (1996) Identification of the primary metal ion-activation sites of the diphtheria tox represser by X-ray crystallography and site-directed mutational analysis. *Nat. Struct. Mol. Biol. 3*, 382−387.
(19) Guedon, E., and Helmann, J. D. (2003) Origins of metal ion selectivity in the DtxR/MntR family of metalloregulators. *Mol. Microbiol. 48*, 495−506.
(20) Rawat, M., and Av-Gay, Y. (2007) Mycothiol-dependent proteins in actinomycetes. *FEMS Microbiol. Rev. 31*, 278−292.
(21) Noszál, B., Visky, D., and Kraszni, M. (2000) Population, Acid−Base, and Redox Properties of *N*-Acetylcysteine Conformers. *J. Med. Chem. 43*, 2176−2182.
(22) Newton, G. L., Arnold, K., Price, M. S., Sherrill, C., Delcardayre, S. B., Aharonowitz, Y., Cohen, G., Davies, J., Fahey, R. C., and Davis, C. (1996) Distribution of thiols in microorganisms: Mycothiol is a major thiol in most actinomycetes. *J. Bacteriol. 178*, 1990−1995.
(23) Grabski, A., Mehler, M., and Drott, D. (2005) The Overnight Express Autoinduction System: High-density cell growth and protein expression while you sleep. *Nat. Methods 2*, 233−235.
(24) Nakamoto, K. (1960) Ultraviolet Spectra and Structures of 2,2′-bipyridine and 2,2′,2″-terpyridine in aqueous Solution. *J. Phys. Chem. 64*, 1420−1425.
(25) Demeler, B. (2012) *UltraScan version 9.9. A Comprehensive Data Analysis Software Package for Analytical Ultracentrifugation Experiments*, The University of Texas Health Science Center at San Antonio, San Antonio, TX.
(26) Wisedchaisri, G., Holmes, R. K., and Hol, W. G. J. (2004) Crystal Structure of an IdeR-DNA Complex Reveals a Conformational Change in Activated IdeR for Base-specific Interactions. *J. Mol. Biol. 342*, 1155−1169.
(27) Jefferson, J. R., Hunt, J. B., and Ginsburg, A. (1990) Characterization of indo-1 and quin-2 as spectroscopic probes for Zn^{2+}-protein interactions. *Anal. Biochem. 187*, 328−336.
(28) Walkup, G. K., and Imperiali, B. (1997) Fluorescent Chemosensors for Divalent Zinc Based on Zinc Finger Domains. Enhanced Oxidative Stability, Metal Binding Affinity, and Structural and Functional Characterization. *J. Am. Chem. Soc. 119*, 3443−3450.
(29) Semavina, M., Beckett, D., and Logan, T. M. (2006) Metal-Linked Dimerization in the Iron-Dependent Regulator from *Mycobacterium tuberculosis*. *Biochemistry 45*, 12480−12490.
(30) Goranson-Siekierke, J., Pohl, E., Hol, W. G., and Holmes, R. K. (1999) Anion-coordinating residues at binding site 1 are essential for the biological activity of the diphtheria toxin repressor. *Infect. Immun. 67*, 1806−1811.
(31) Rangachari, V., Marin, V., Bienkiewicz, E. A., Semavina, M., Guerrero, L., Love, J. F., Murphy, J. R., and Logan, T. M. (2005) Sequence of Ligand Binding and Structure Change in the Diphtheria Toxin Repressor upon Activation by Divalent Transition Metals. *Biochemistry 44*, 5672−5682.
(32) Brumas, V., Hacht, B., Filella, M., and Berthon, G. (1992) Can N-acetyl-L-cysteine affect zinc metabolism when used as a paracetamol antidote? *Agents Actions 36*, 278−288.

(33) De la Torre, J. G., Huertas, M. L., and Carrasco, B. (2000) Calculation of hydrodynamic properties of globular proteins from their atomic-level structure. *Biophys. J. 78*, 719−730.
(34) Rai, N., Nollmann, M., Spotorno, B., Tassara, G., Byron, O., and Rocco, M. (2005) SOMO(SOlution MOdeler): Differences between X-ray- and NMR-derived bead models suggest a role for side chain flexibility in protein hydrodynamics. *Structure 13*, 723−734.
(35) Twigg, P. D., Parthasarathy, G., Guerrero, L., Logan, T. M., and Caspar, D. L. D. (2001) Disordered to ordered folding in the regulation of diphtheria toxin repressor activity. *Proc. Natl. Acad. Sci. U.S.A. 98*, 11259−11264.
(36) Pohl, E., Holmes, R. K., and Hol, W. G. J. (1999) Crystal Structure of the Iron-dependent Regulator (IdeR) from *Mycobacterium tuberculosis* Shows Both Metal Binding Sites Fully Occupied. *J. Mol. Biol. 285*, 1145−1156.
(37) Feese, M. D. (2000) Crystal Structure of the Iron-dependent Regulator from *Mycobacterium tuberculosis* at 2.0-Å Resolution Reveals the Src Homology Domain 3-like Fold and Metal Binding Function of the Third Domain. *J. Biol. Chem. 276*, 5959−5966.
(38) Boyd, J., Oza, M. N., and Murphy, J. R. (1990) Molecular cloning and DNA sequence analysis of a diphtheria tox iron-dependent regulatory element (dtxR) from *Corynebacterium diphtheriae*. *Proc. Natl. Acad. Sci. U.S.A. 87*, 5968−5972.
(39) VanZile, M. L., Cosper, N. J., Scott, R. A., and Giedroc, D. P. (2000) The Zinc Metalloregulatory Protein *Synechococcus* PCC7942 SmtB Binds a Single Zinc Ion per Monomer with High Affinity in a Tetrahedral Coordination Geometry. *Biochemistry 39*, 11818−11829.
(40) Kar, S. R., Adams, A. C., Lebowitz, J., Taylor, K. B., and Hall, L. M. (1997) The Cyanobacterial Repressor SmtB Is Predominantly a Dimer and Binds Two Zn^{2+} Ions per Subunit. *Biochemistry 36*, 15343−15348.
(41) Love, J. F., VanderSpek, J. C., Marin, V., Guerrero, L., Logan, T. M., and Murphy, J. R. (2004) Genetic and biophysical studies of diphtheria toxin repressor (DtxR) and the hyperactive mutant DtxR (E175K) support a multistep model of activation. *Proc. Natl. Acad. Sci. U.S.A. 101*, 2506−2511.
(42) Demeler, B., Saber, H., and Hansen, J. C. (1997) Identification and interpretation of complexity in sedimentation velocity boundaries. *Biophys. J. 72*, 397−407.
(43) Wagner, D., Maser, J., Lai, B., Cai, Z., Barry, C. E., III, Höner Zu Bentrup, K., Russell, D. G., and Bermudez, L. E. (2005) Elemental analysis of *Mycobacterium avium*-, *Mycobacterium tuberculosis*-, and *Mycobacterium smegmatis*-containing phagosomes indicates pathogen-induced microenvironments within the host cell's endosomal system. *J. Immunol. 174*, 1491−1500.
(44) Dokmanić, I., Šikić, M., and Tomić, S. (2008) Metals in proteins: Correlation between the metal-ion type, coordination number and the amino-acid residues involved in the coordination. *Acta Crystallogr. D64*, 257−263.
(45) Busenlehner, L. S., Weng, T.-C., Penner-Hahn, J. E., and Giedroc, D. P. (2002) Elucidation of primary (α(3)N) and vestigial (α(5)) heavy metal-binding sites in *Staphylococcus aureus* pI258 CadC: Evolutionary implications for metal ion selectivity of ArsR/SmtB metal sensor proteins. *J. Mol. Biol. 319*, 685−701.
(46) Lee, J.-W. (2006) Biochemical Characterization of the Structural Zn^{2+} Site in the *Bacillus subtilis* Peroxide Sensor PerR. *J. Biol. Chem. 281*, 23567−23578.
(47) Vitale, S., Fauquant, C., Lascoux, D., Schauer, K., Saint-Pierre, C., and Michaud-Soret, I. (2009) A ZnS4 Structural Zinc Site in the *Helicobacter pylori* Ferric Uptake Regulator. *Biochemistry 48*, 5582−5591.
(48) Gresits, I., and Könczöl, K. (2003) Determination of trace elements in *Mycobacterium fortuitum* by X-ray fluorescence spectrometry. *X-ray Spectrom. 32*, 413−417.
(49) Pihl, E., Gustafson, G. T., Josefsson, B., and Paul, K.-G. (1967) Heavy Metals in the Granules of Eosinophilic Granulocytes. *Scand. J. Haematol. 4*, 371−379.
(50) Eide, D. J. (2006) Zinc transporters and the cellular trafficking of zinc. *Biochim. Biophys. Acta 1763*, 711−722.
(51) Serafini, A., Boldrin, F., Palù, G., and Manganelli, R. (2009) Characterization of a *Mycobacterium tuberculosis* ESX-3 Conditional Mutant: Essentiality and Rescue by Iron and Zinc. *J. Bacteriol. 191*, 6340−6344.
(52) Maciag, A., Dainese, E., Rodriguez, G. M., Milano, A., Provvedi, R., Pasca, M. R., Smith, I., Palu, G., Riccardi, G., and Manganelli, R. (2006) Global Analysis of the *Mycobacterium tuberculosis* Zur (FurB) Regulon. *J. Bacteriol. 189*, 730−740.
(53) Reyes-Caballero, H., Campanello, G. C., and Giedroc, D. P. (2011) Metalloregulatory proteins: Metal selectivity and allosteric switching. *Biophys. Chem. 156*, 103−114.